Electronic Supplementary Material (ESI) for Journal of Materials Chemistry B.
This journal is © The Royal Society of Chemistry 2019

Supporting information

Polysaccharide-Based Recoverable Double-Network Hydrogel with High Strength and Self-healing Property

Kun Lei,[a+] Zhao Li,[b+] Dandan Zhu,[a] Chengyuan Sun,[a] Yunlong Sun,[a] Chongchong Yang,[a] Zhen Zheng,[a] and Xinling Wang[a*]

[a] School of Chemistry and Chemical Engineering, Shanghai Jiao Tong University, Shanghai 200240, China. e-mail: xlwang@sjtu.edu.cn

[b] Institute of Engineering Medicine, Beijing Institute of Technology, Beijing, 100081, P. R. China.

Corresponding author: Xinling Wang

E-mail: xlwang@sjtu.edu.cn

Contents

1.12. In Vitro Cell Viability Assay.

1.13. Cell adhesion Test.

1.14. Functionalization of Gels.

1.15. Statistical Analysis.

Figure S1. Structure of SA-CHO/Aga DN gel. (a) Schematics and construction of the SA-CHO/Aga DN gel. (b) Stability of SA-CHO and SA-CHO/Aga DN gel.

Figure S2. Compressive experiments of SA-CHO gels with different content of SA-CHO: (a) 4%; (b) 6%; (c) 8%; (d) 10%.

Figure S3. Compressive experiments of SA-CHO/Aga DN gels with different content of SA-CHO: (a) 4%; (b) 6%; (c) 8%; (d) 10%.

Figure S4. Compressive experiment of pure Aga gel with 2 w/v% content of Aga

Figure S5. Compressive experiments of DN gels with different content of Aga: (a) 0%; (b) 0.5%; (c) 1.0%; (d) 1.5%; (e) 2.0%

Figure S6. Compressive experiments of DN gels with different content of Aga: (a) fracture stress, and strain; (b) compressive modulus. (Values were presented as mean ± standard deviation, n = 4).

Figure S7. (a) The mean scattering intensity of SA-CHO/Aga DN gels at various SA-CHO contents. The images of the DN gels when the SA-CHO contents are (b) 4, (c) 6, (d) 8, (e) 10 w/v%. The compression pictures of gels: Aga gel (f) before, (g) after compression; SA-CHO/Aga DN gel (h) before, (i) after compression. (Values were presented as mean ± standard deviation, n = 4).

Figure S8. Tensile properties of DN gels with different content of SA-CHO: stress-strain curves (a); fracture tensile stress (b); tensile modulus (c). (Values were presented as mean ± standard deviation, n = 4).

Figure S9. Compression modulus ratio of the third and the first loading (E_{third}/E_{first}) as a function of different compressive strain (8% DN gel).

Figure S10. Rheology tests of SA-CHO/Aga DN gels with (a) 10%, (b) 8%, (c) 6%, and (d) 4 w/v% of SA-CHO concentration at T=20-120 °C and strain (γ) = 1%.

Figure S11. Temperature (t) sweep experiment at t = 20-120 ^{0}C, and strain (γ) = 1% of 2 w/v% of (a) 2% concentration of Aga gel; (b) 4% content of SA-CHO gel.

Figure S12. Self-healing tests of the Aga gel or DN gels formed in aqueous buffers of pH (a) Aga gel, (b) 7.4, (c) 8.5, (d) 10.5, (e) 11.5, (f) 7.4+4.5, and (g) DN gel formed in an aqueous buffer solution of pH 7.4 after the addition of a small volume of an aqueous buffer solution of pH 4.5 (The concentration of SA-CHO is 8 w/v%).

Figure S13. Cytotoxicity test of SA-CHO, DN, and Aga gels leachable solutions with L929 fibroblast cells. (Values were presented as mean ± standard deviation, n = 3).

Figure S14. Synthesis and characterization of SA-CHO. (a) Schematic and structure of SA-CHO;

(b) FTIR spectra of SA, and SA-CHO; (c) ^{1}HNMR spectra of SA, and SA-CHO; (d) Hydroxylamine hydrochloride potentiometric titration of various SA-CHO samples; (e) Oxidation degree (mol%)

Figure S15. Tube inversion tests demonstrating the fabrication of SA-CHO/Aga DN gels (10% DN gel) within the pH range 2.0-11.5. (a) Before the gelation. (b) After the gelation. Different coloration is attributed to the existence of some traces of dye.

Figure S16. Temporal changes of the G' and G'' during the formation of the SA-CHO/Aga DN gels (10% DN gel) at 50 ℃ in PBS solution with various pH values (a) 1.0, (b) 11.5, (c) 2.0, and (d) 7.4.

Figure S17. Swelling behavior of gels in acidic condition (pH=1). (a) The swelling behavior of the SA-CHO gel. (b) Pictures of the SA-CHO gel's form change. (c) The swelling behavior of the DN gel. (d) Pictures of the DN gel's form change. (e) The swelling behavior of the Aga gel. (f) Pictures of the Aga gel's form change. (Values were presented as mean ± standard deviation, n = 4).

Figure S18. Swelling behavior of gels in DI water. (a) The swelling behavior of the SA-CHO gel. (b) Pictures of the SA-CHO gel's form change. (c) The swelling behavior of the DN gel. (d) Pictures of the DN gel's form change. (e) The swelling behavior of the Aga gel. (f) Pictures of the Aga gel's form change. (Values were presented as mean ± standard deviation, n = 4).

Figure S19. (a) UV-visible spectra of the gel after functionalization for different time, (b) Fluorescence yield (W_{ti}) of aminopyrene in DN gel functionalized for different time. Pictures of DN gels under visible light (c), and UV-visible light (d).

1.1. Materials and Chemicals. Sodium alginate (SA) was purchased from Adamas Reagent Co., Ltd (~250 kDa, 99.8%). Agarose (CAS: 9012-36-6, congealing temperature between 32 and 35 ^{0}C) was obtained from Sigma-Aldrich Co., Ltd (~ 150 kDa, 99.9%). Adipic dihydrazide (ADH, 99.9%) was obtained from Sigma-Aldrich Co., Ltd. 1-Pyrenamine (99.8%) was purchased from Tokyo Chemical Industry. All reagents were used as received without any treatment.

1.2. Preparation of Oxidized Sodium Alginate. SA-CHO was prepared to attain aldehyde form according to described method previously.[1,2] Briefly, 5.0 g SA was dissolved in 50 mL distilled water, and then 50 mL $NaIO_4$ solution with 0.8 of molar ratio of $NaIO_4$ to saccharide repeating units of SA was added. The oxidation reaction processed in the dark environment at room temperature for 4h. The reaction was terminated by adding excess amount of ethylene glycol and kept for 30 min again, followed by the dialysis against distilled water for 3 days. Finally, the purified SA-CHO product was obtained by lyophilization.

The aldehyde group content (the molar amount of aldehyde group in each unit mass of SA-CHO, in mol/g), and the oxidation degree of SA-CHO (percentage of oxidized

sodium alginate saccharide repeating units) were determined through measuring the volume of consumed sodium hydroxide solution using hydroxylamine hydrochloride titration means.[3] 0.1g lyophilized SA-CHO was dissolved in 25 mL of 0.25 mol/L hydroxylamine hydrochloride solution (pH kept to 4.5) containing 0.001 wt % methyl orange reagent. The solution was stirred at room temperature for 12 h. Then, the mixture containing the released HCl after the reaction of aldehydes into oximes was titrated by sodium hydroxide solution (0.1 mol/L) until the color of the solution changed from red to yellow. The variation of pH with the volume of added NaOH solution was recorded. The relevant chemical reaction and calculation formulas are shown as follows:

$$\text{SA-(CHO)}_n + n\text{H}_2\text{N-OH}\cdot\text{HCl} = \text{SA-(CH=N-OH)}_n + n\text{H}_2\text{O} + n\text{HCl} \quad (1)$$

$$\text{HCl} + \text{NaOH} = \text{NaCl} + \text{H}_2\text{O} \quad (2)$$

$$[\text{CHO}] = \Delta V \times c \times 10^{-3}/\text{w}$$

$$\text{OD} = 198\Delta V \times c \times 10^{-3}/2\text{w}$$

Where [CHO] refers to the aldehyde group content, in mol/g; OD refers to the oxidation degree of SA-CHO; ΔV is the consumed volume of NaOH solution, in mL; c is the concentration of NaOH solution, in mol/L; w is the weight of SA-CHO, in g; and 198 is the molecular weight of sodium alginate repeating units, in g/mol.

1.3. Preparation of SA-CHO and SA-CHO/Aga DN Hydrogels. The SA-CHO/Aga DN hydrogels were prepared by mixing the phosphate buffer solutions (PBS) of the SA-CHO and the ADH in 2 w/v% agarose solution (both compounds in buffer solutions with the same pH) at the equal molar ratio of aldehyde group and hydrazide group. The preparation was conducted in seven different PBS (150 mM) with pH values of 2.0, 4.5, 7.4, 8.5, 10.5, and 11.5. In a typical example, agarose (100 mg) was added into a vial with 5 mL of PBS (pH=7.4) and heated to 120 °C for 10 min to form a transparent solution (2 w/v% in concentration). The transparent agarose solution was cooled to 50 °C for use. With the above agarose solution of SA-CHO (1 mL) with 4%, 6%, 8%, and 10% (w/v) of SA-CHO concentration, the prepared agarose solution of ADH (0.5 mL, molar ratio of hydrazide group in ADH and aldehyde group in SA-CHO equal to 1) was mixed and the mixture was gently vortexed at 50 °C until the gel was obtained. Then the gel was cooled down at room temperature and kept for 48 h to make the DN hydrogels form completely. The final concentrations of SA-CHO were 2.7%, 4%, 5.4%, and 6.7% (w/v) in the SA-CHO/Aga DN hydrogels, respectively. Here, the corresponding hydrogels are abbreviated as 4% DN gel, 6% DN gel, 8% DN gel, and 10% DN gel based on the concentration of SA-CHO in agarose solution before the mixing. The water content of the gels for 4% DN gel, 6% DN gel, 8% DN gel, and 10%

DN gel is 95.5%, 94.3%, 93.2%, and 92%, respectively. The time to form a gel (denoted as gelation time) was determined using the vial tilting way. No flow within 1 min upon inverting the vial was regarded as the gel state. The above process was operated using all six PBS with different pH. Similarly, pristine SA-CHO hydrogels were prepared by mixing SA-CHO and ADH in PBS without the addition of agarose. The hydrogel could be molded into any shape according to the requirements, for example cylindrical shape, star shape, etc.

1.4. Mechanical Properties Measurements. The compressive performances of the hydrogels are measured using a universal testing machine (Model 43 MTS Criterion). Hydrogels were prepared in cylindroid molds (a size of 14 mm in diameter and 7 mm in height). The dimensions of each sample were determined using a digital caliper before compressive experiment. The rate of compression testing was kept at 1 mm/min until the sample ruptured. The SA-CHO hydrogels without agarose were utilized as the control. In the same kind of sample, the testing was performed four times, and the averages with standard deviations were reported. For tensile assays, the gels were cut into dumbbell shapes (GBT 528-20094) of a size of 10x2 x2 mm^3 with 25 mm/min of strain rate. Similarly. The tests were repeated four times and the averages with standard deviations were reported.

1.5. Cyclic Compression Test. Cyclic compression tests were operated on MTS Criterion 43 universal testing machine at room temperature. Both loading and unloading were performed at a constant compression rate of 5 mm min^{-1}. In the loading-unloading cycles, the sample was compressed to a strain of 80% and then relaxed at room temperature. For recovery tests, the samples were firstly performed by a loading cycle to achieve a compression of 70%, and then the specimens were sealed in the plastic tube and disposed at 50 ^{0}C with 5, 15 min, and 120 ^{0}C with 5, 10, and 30 min. Finally, the samples were taken out at different time intervals and cooled down to room temperature for experiments.

1.6. Swelling and Stability Properties of the Gels. To demonstrate the stability properties of the hydrogels in acid aqueous solution, the above attained hydrogels without lyophilization (SA-CHO/Aga DN, SA-CHO, Aga) were immersed into hydrochloric acid aqueous solution (pH=1). After a period of time, the swollen hydrogels were taken out from the hydrochloric acid aqueous solution. Subsequently, the water was removed from the surface of the swollen hydrogels using filter paper. The weights of initial hydrogels (W_0) and swollen hydrogels (W_s) were recorded at 25 °C. The remaining mass was calculated using the following equation:

$$Remaining\ mass = \frac{W_S}{W_0} \times 100\% \quad (3)$$

Stability properties of hydrogels in DI water were also examined as the same as the above procedure. Then, equation 3 was also used to calculate the remaining mass in DI water. The tests were repeated four times and the averages with standard deviations are reported.

1.7. Fourier Transform Infrared Spectra. The FTIR spectra of SA-CHO, SA-CHO hydrogel, SA-CHO/Aga DN hydrogel, and Aga hydrogel were recorded on a Paragon 1000 instrument (Perkin Elmer, Inc., USA). The scan range was 4000 to 500 cm^{-1} with a resolution of 2 cm^{-1}. Before testing, the SA-CHO hydrogel, SA-CHO/Aga hydrogel DN hydrogel, Aga hydrogel were formed according to the above mentioned methods and then lyophilized at -40 °C for 72 h.

1.8. Hydrogen Nuclear Magnetic Resonance. The formation of SA-CHO and acyl hydrazone bond after the reaction between SA-CHO and ADH was characterized by ^{1}HNMR. The ^{1}HNMR spectra were obtained by a Mercuryplus 500 NMR from Varian at 25.0 ± 0.5 ℃. Deuterated water (D_2O) was used as solvent for all the samples. The signal of solvent residue was used as reference peak for the ^{1}HNMR chemical shift and was set at δ 4.79 for water.

1.9. Rheological Characterization. The rheological behaviors of the SA-CHO/Aga DN hydrogels are determined using an AR-G2 Rheometer (TA Instruments, USA). The rheometer was conducted in three different kinds of oscillatory mode, including the time (t)-dependent oscillatory mode, the angular frequency (ω)-dependent oscillatory mode, and the temperature (T)-dependent oscillatory mode. For the time-dependent oscillatory rheology measurements with ω of 10 rad s^{-1}, 1% strain, 1 mL of 10% w/v agarose solution of SA-CHO and the prepared agarose solution of ADH (0.5 mL, molar ratio of hydrazide group in ADH and aldehyde group in SA-CHO equal to 1) were mixed together and transferred at once on the bottom rheometer plate. Four different aqueous buffer solutions at pH= 1.0, 2.0, 7.4 and 11.5 are used to perform the tests until all the gels were formed within 10 min (the gelation time was measured by the tube inversion experiments). In rheology, the judgement standard for gel formation was the intersection point of the rheological curves for the two modulus, the storage modulus G' and the loss modulus G''. For the angular frequency (ω) sweep test measurements, gel samples with a 25 mm diameter and a 3 mm height were obtained in PBS at pH=1.5, 2.0, 4.5 and 7.4, and conducted at angular frequency (ω) = 0.01−100 rad/s and strain (γ) = 1% at 25 ^{0}C. The temperature (T) oscillatory tests for 4% DN gel, 6% DN gel, 8% DN gel, and 10% DN gel were operated at T=20-120 ^{0}C with strain (γ) = 1% and angular

frequency (ω) =1 rad/s; in order to avoid the dehydration of samples during measurement, the surrounding of samples was sealed a thin layer of silicone oil with 20 ^{0}C/min of the heating rate. For the temperature oscillatory tests, every gel sample was performed in triplicate.

1.10. Dynamic Light Scattering Measurements. The dynamic light scattering (DLS) tests were performed on the DLS Spectrometer from Malvern Instruments Ltd consisting of a goniometer system with the incident light of 632.8 nm according to the literature reported by others.[4] The tests are conducted at a 90° angle with the temperature of 50 ^{0}C. The measured samples are prepared by mixing the SA-CHO and ADH agarose solution. The tests were repeated four times and the averages with standard deviations are reported.

1.11. Self-Healing Experiments. First, the SA-CHO (1.0 mL, 0.08 g) and the ADH (0.5 mL, 0.03 g) were separately dissolved in agarose buffer solution (150 mM) of pH 7.4, at the stoichiometric ratio of hydrazide group in ADH and aldehyde group in SA-CHO. Then, the two compound solutions were mixed together at 25 ℃ with the final 5.4 w/v% of SA-CHO concentration. The same step was also carried out using the five other PBS of pH 2.0, 4.5, 8.5, 10.5, and 11.5. After the gelation, every SA-CHO/Aga DN hydrogel was cut into two pieces. The cut surfaces of the two gel pieces were brought into contact and maintained together for 48 h without other stress or outside stimulus.

Besides, another 8% DN gel was also prepared at an aqueous buffer of pH 7.4 and the hydrogel was immersed in large amounts of water until a balance was achieved. During the period, the water was exchanged several times to remove any traces of the phosphate salts. Then, the 8% DN gel was cut into two pieces. One was immersed to swell in deionized water, and the other was immersed to swell in deionized water of the Rhodamine B. After 12 h, the two pieces were placed on a glass culture dish, and a catalyzed amount of PBS with pH 4.5 was added on the SA-CHO/Aga DN hydrogel cut surface. Subsequently, the cut surfaces of the two gel pieces were brought into contact and maintained for 48 h.

In addition, the DN hydrogel sample prepared at pH 7.4 was pressed together with those prepared at pH 2.0 and 4.5 to investigate whether the two pieces were endowed with self-healing ability.

1.12. In *Vitro* Cell Viability Assay. The Cell Viability test was determined according to quantitative MTT cytotoxicity assay utilizing L929 mouse fibroblasts and was assessed by contacting extracts of the hydrogels. Specifically, L929 cells were

suspended in cell culture medium and seeded into 96-well plates at a density of 1×10^5 cells per well, being incubated for 24 h at 37 °C in 5% CO_2 to obtain a monolayer of cells. Hydrogel extracts were obtained by adding 1 g 10% DN gel fragments to 10 mL DMEM culture medium and being soaked at 37 °C for 24 h. After then, the residual DN hydrogels were removed. Subsequently, cell medium was substituted by above hydrogel extracts and further incubated for 1, 2, 3 days. The sample solution was extracted after incubation and the cells were further incubated with 50 μL of 1 mg/mL of MTT solution for 4h. Finally, the culture medium was displaced with 150 μL of DMSO to dissolve the formed formazan and the absorbance of the DMSO solution at 570 nm was measured by a microplate reader (Synergy HT). The relative cell viability was calculated as the ratio between the mean absorbance value of the sample and that of cells cultured in the pure DMEM. The experiment was examined three times for each culture. Values were shown as mean ± standard deviation (n = 3). The samples with relative cell viability more than 70% were considered to be non-cytotoxic. Similarly, the in vitro cell viability tests of SA-CHO hydrogel, Aga hydrogel are also demonstrated as shown above. The determination was performed in triplicate and the averages with standard deviations are reported.

1.13. Cell adhesion Test. The hydrogel samples were incubated using 2mL of 1×10^5 cells per well suspension of L929 mouse fibroblasts in 6 well plates at 37 °C and 5% CO2. After 2, 4 d, substrate was washed with fresh medium to eliminate un-adhered cells. Cells were digested, and counted utilizing a cell counter. Subsequently, 1.5% FDA solution was used to stain the cells on the hydrogel surface, followed by immobilization with 2% glutaraldehyde. Fluorescence pictures were acquired utilizing a laser confocal microscopy (LCFM). The tests were repeated four times and the averages with standard deviations are reported.

1.14. Functionalization of Hydrogels. 1-Aminopyrene (fluorescent substance) with amino (NH_2) was utilized to modify the hydrogels through Schiff-base reaction. The DN hydrogel was immersed in a DMF solution of 1-Aminopyrene (1.5 mg mL^{-1}) for 24 h at 40 °C to finish the reaction between the remaining aldehyde groups within the hydrogel and the amino groups of 1-Aminopyrene. Then, the hydrogel was washed with excess DMF for 6 h, and excess water for 6 h. During the period, the DMF and water were frequently changed until no UV absorbance of 1-Aminopyrene in DMF was observed by the ultraviolet absorption spectrum. Finally, the hydrogels were directly pictured using a laser confocal microscope (excitation: 365 nm). Besides, a UV/vis spectrophotometer was utilized to determine the absorption spectrum of the

functionalized DN hydrogel. The scan range is 200-600 nm with step of 1.5 nm. PTFE was applied as an absorption standard. A hydrogel sample with diameter of 20 mm and height of 2 mm was sandwiched in two quartz plates. The content of conjugated aminopyrene in the DN hydrogels was defined as fluorescence yield (Wt_i). The absorbance at 287 nm of the functionalized hydrogel with final 6.7 w/v% of SA-CHO for different time was measured. The fluorescence yield (Wt_i) was obtained from a calibration curve attained by examining the absorbance of aminopyrene at different concentrations in DMF. Fluorescence yield (Wt_i) was determined as follows:

$$Wt_i = \frac{c_i}{67} \times 100\% \qquad (4)$$

Here, c_i refers to the concentration of aminopyrene in the functionalized hydrogel for different time, calculated from a calibration curve of aminopyrene, in mg/mL; the number 67 refers to the final concentration of SA-CHO in hydrogel system, in mg/mL, i=0, 4, 8, 12, 16, 20, 24 h.

1.15. Statistical Analysis. The one-way analysis of variance and the t-test were used to determine the statistical significance. A probability (P) value <0.05 was considered significant, and $P<0.01$ was highly significant. All computations were made by employing Microsoft Excel 2013.

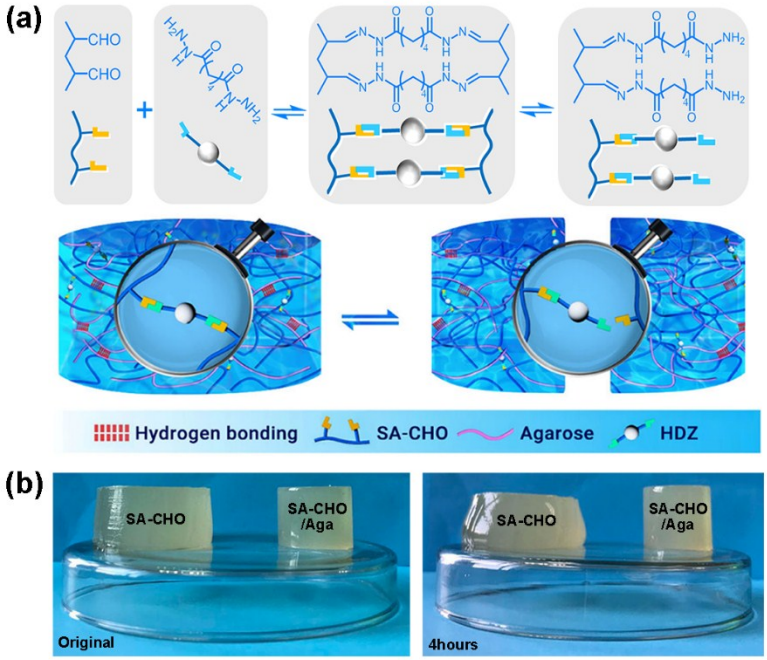

Figure S1. Structure of SA-CHO/Aga DN gel. (a) Schematics and construction of the SA-CHO/Aga DN gel. (b) Stability of SA-CHO and SA-CHO/Aga DN gel.

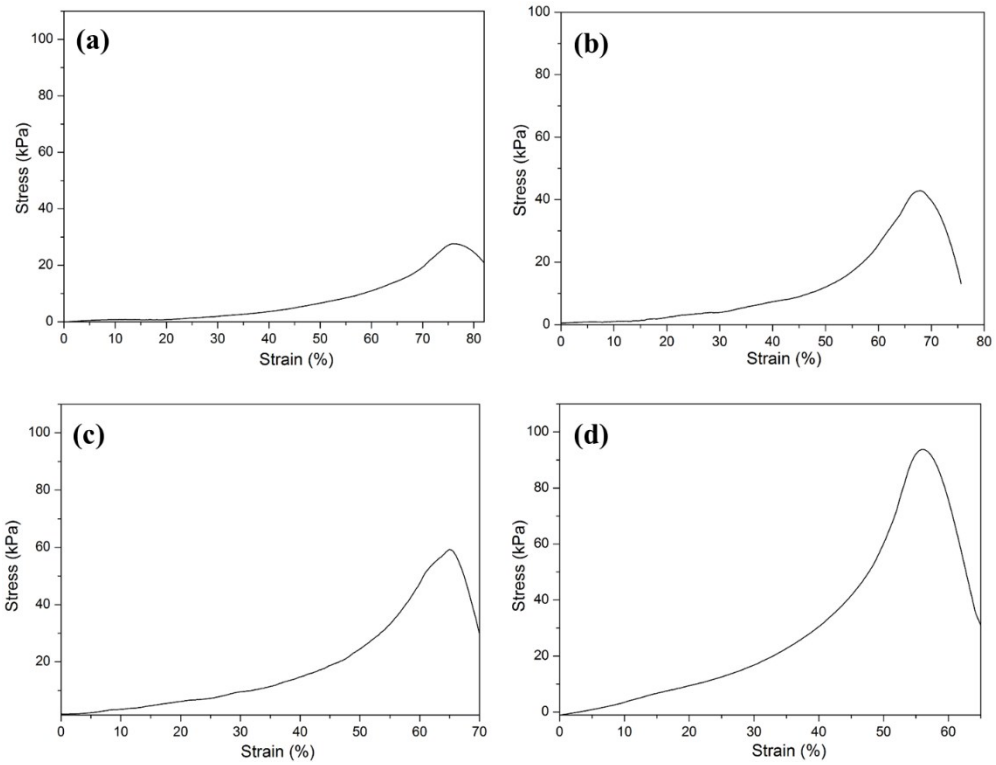

Figure S2**.** Compressive experiments of SA-CHO gels with different content of SA-CHO: (a) 4%; (b) 6%; (c) 8%; (d) 10%.

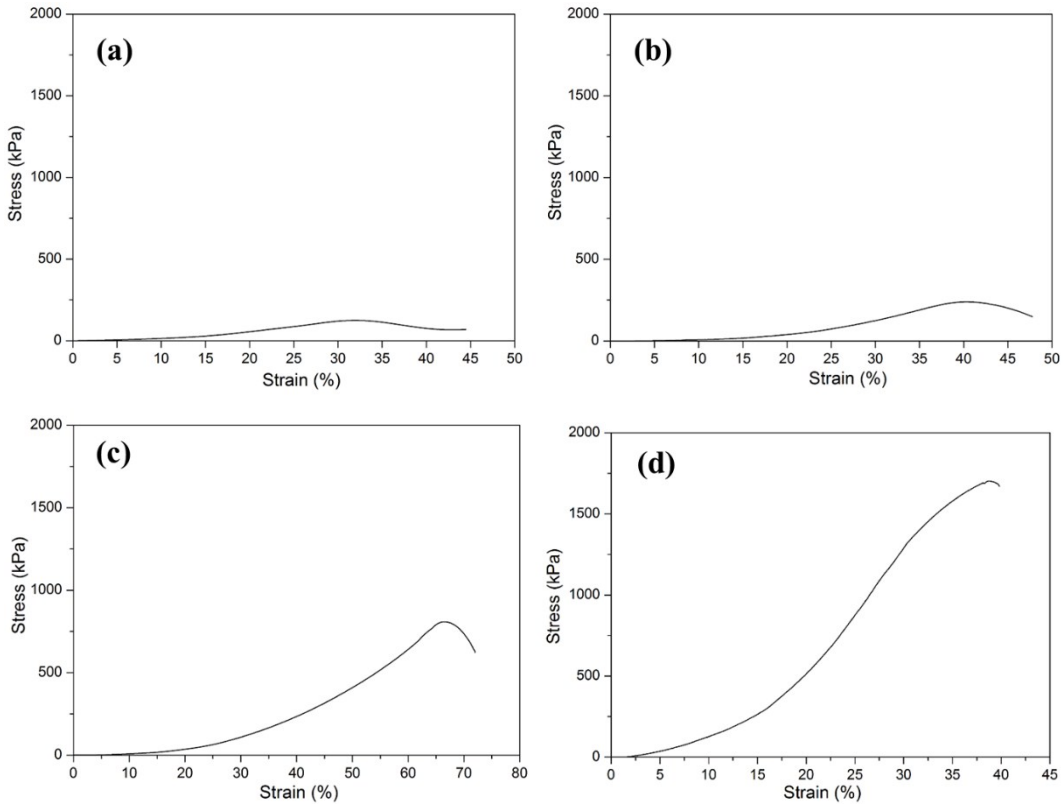

Figure S3**.** Compressive experiments of SA-CHO/Aga DN gels with different content of SA-CHO:

(a) 4%; (b) 6%; (c) 8%; (d) 10%.

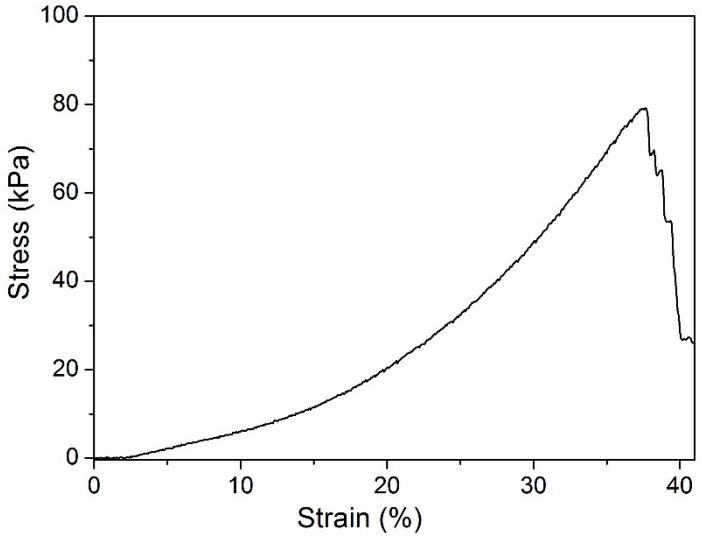

Figure S4**.** Compressive experiment of pure Aga gel with 2 w/v% content of Aga

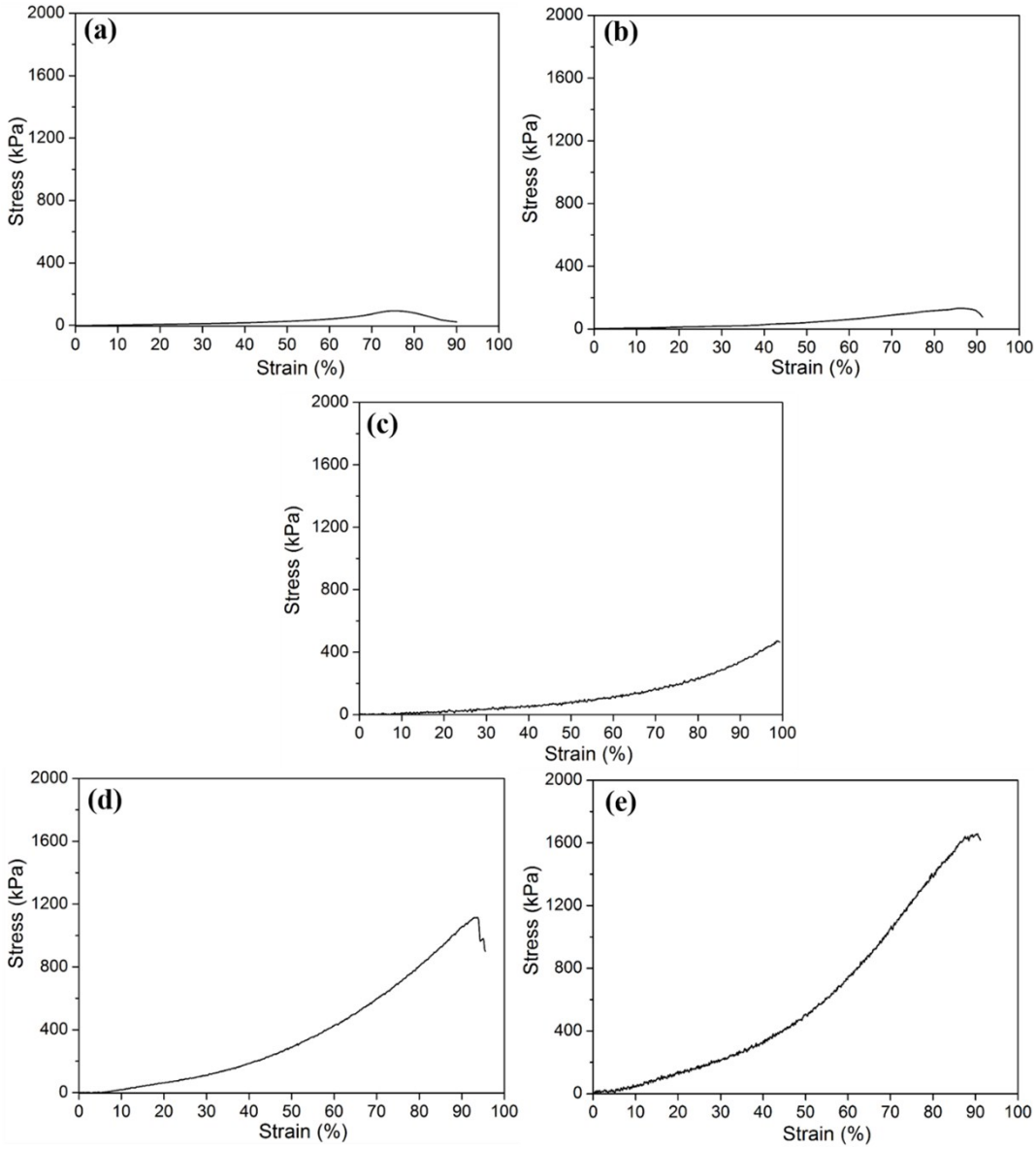

Figure S5**.** Compressive experiments of DN gels with different content of Aga: (a) 0%; (b) 0.5%; (c) 1.0%; (d) 1.5%; (e) 2.0%

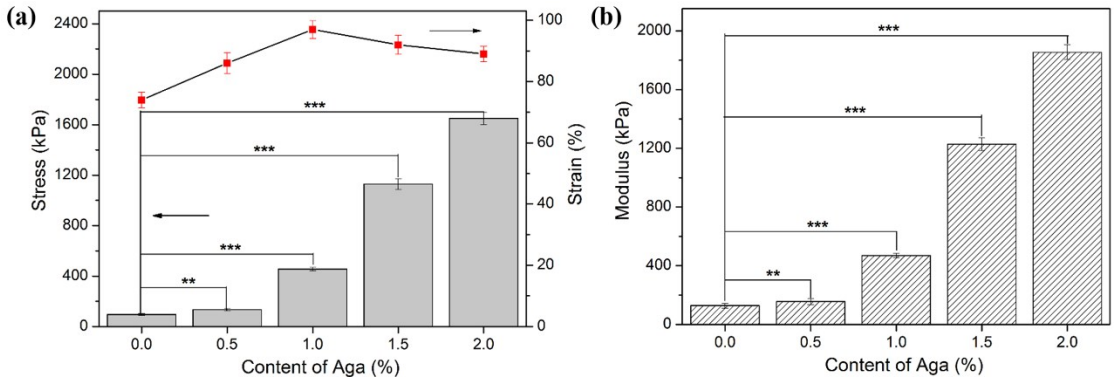

Figure S6**.** Compressive experiments of DN gels with different content of Aga: (a) fracture stress,

and strain; (b) compressive modulus. (Values were presented as mean ± standard deviation, n = 4; $P^{**}<0.05$, $P^{***}<0.01$).

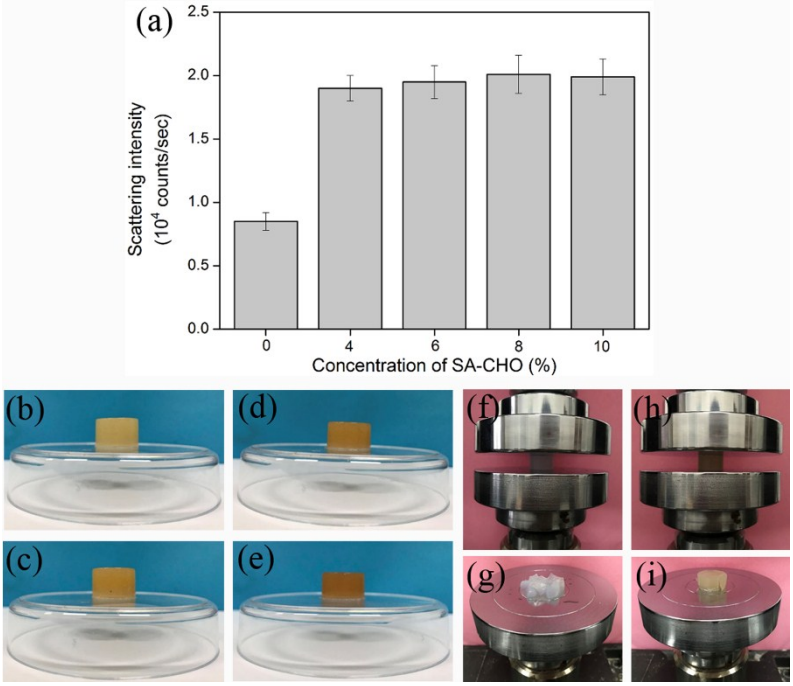

Figure S7**.** (a) The mean scattering intensity of SA-CHO/Aga DN gels at various SA-CHO contents. The images of the DN gels when the SA-CHO contents are (b) 4, (c) 6, (d) 8, (e) 10 w/v%. The compression pictures of gels: Aga gel (f) before, (g) after compression; SA-CHO/Aga DN gel (h) before, (i) after compression. (Values were presented as mean ± standard deviation, n = 4).

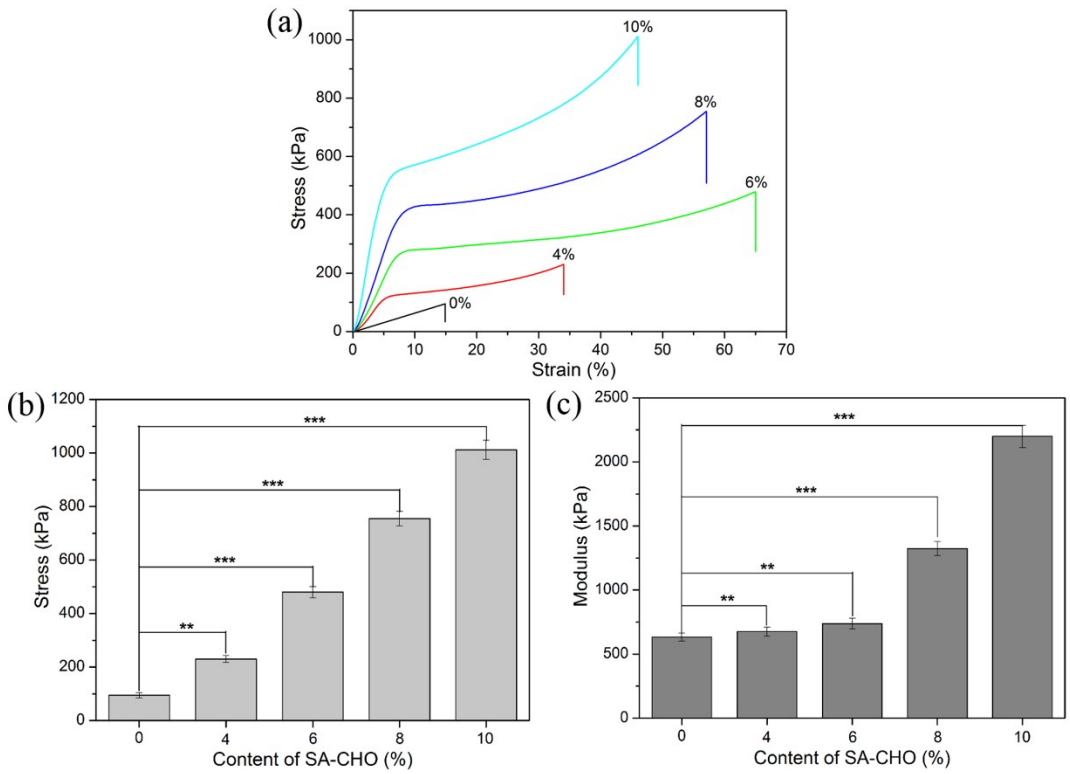

Figure S8. Tensile properties of DN gels with different content of SA-CHO: stress-strain curves (a); fracture tensile stress (b); tensile modulus (c). (Values were presented as mean ± standard deviation, n = 4; $P^{**}<0.05$, $P^{***}<0.01$).

Note: concentration of SA-CHO refers to the amount of SA-CHO in Aga solution before the mixing.

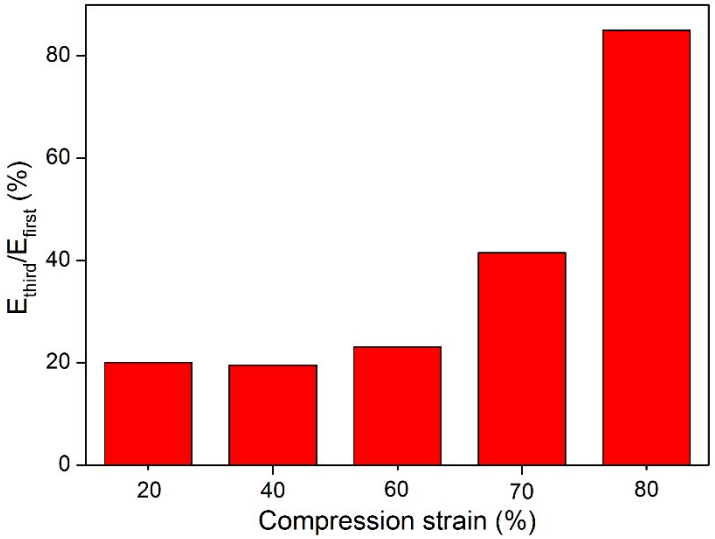

Figure S9**.** Compression modulus ratio of the third and the first loading (E_{third}/E_{first}) as a function of different compressive strain (8% DN gel).

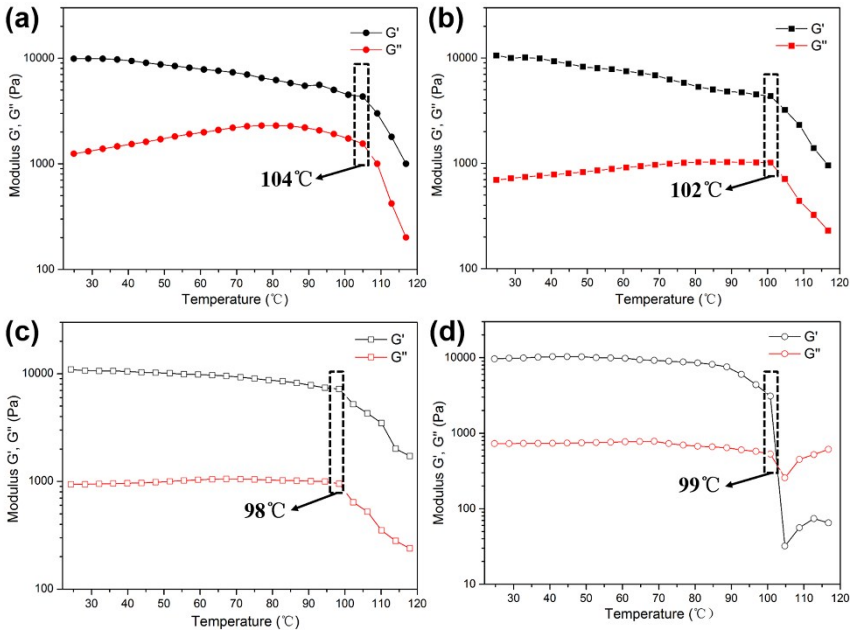

Figure S10**.** Rheology tests of SA-CHO/Aga DN gels with (a) 10%, (b) 8%, (c) 6%, and (d) 4 w/v% of SA-CHO concentration at T=20-120 °C and strain (γ) = 1%.

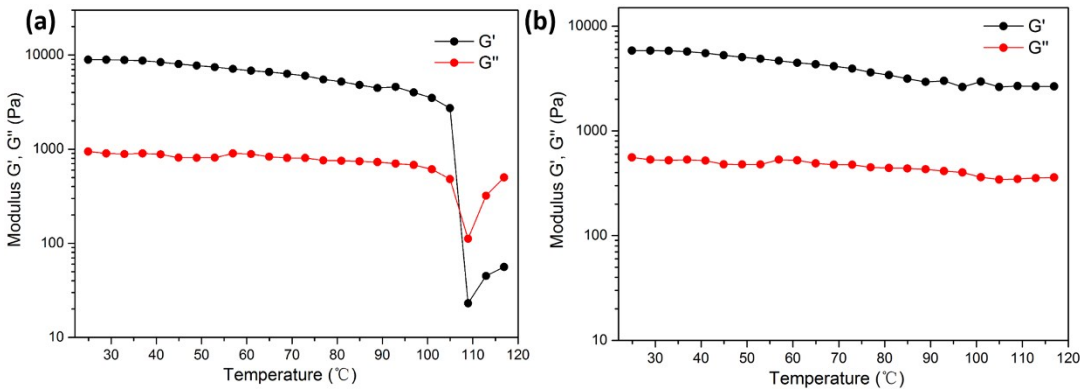

Figure S11**.** Temperature (t) sweep experiment at t = 20-120 ^{0}C, and strain (γ) = 1% of 2 w/v% of (a) 2% concentration of Aga gel; (b) 4% content of SA-CHO gel.

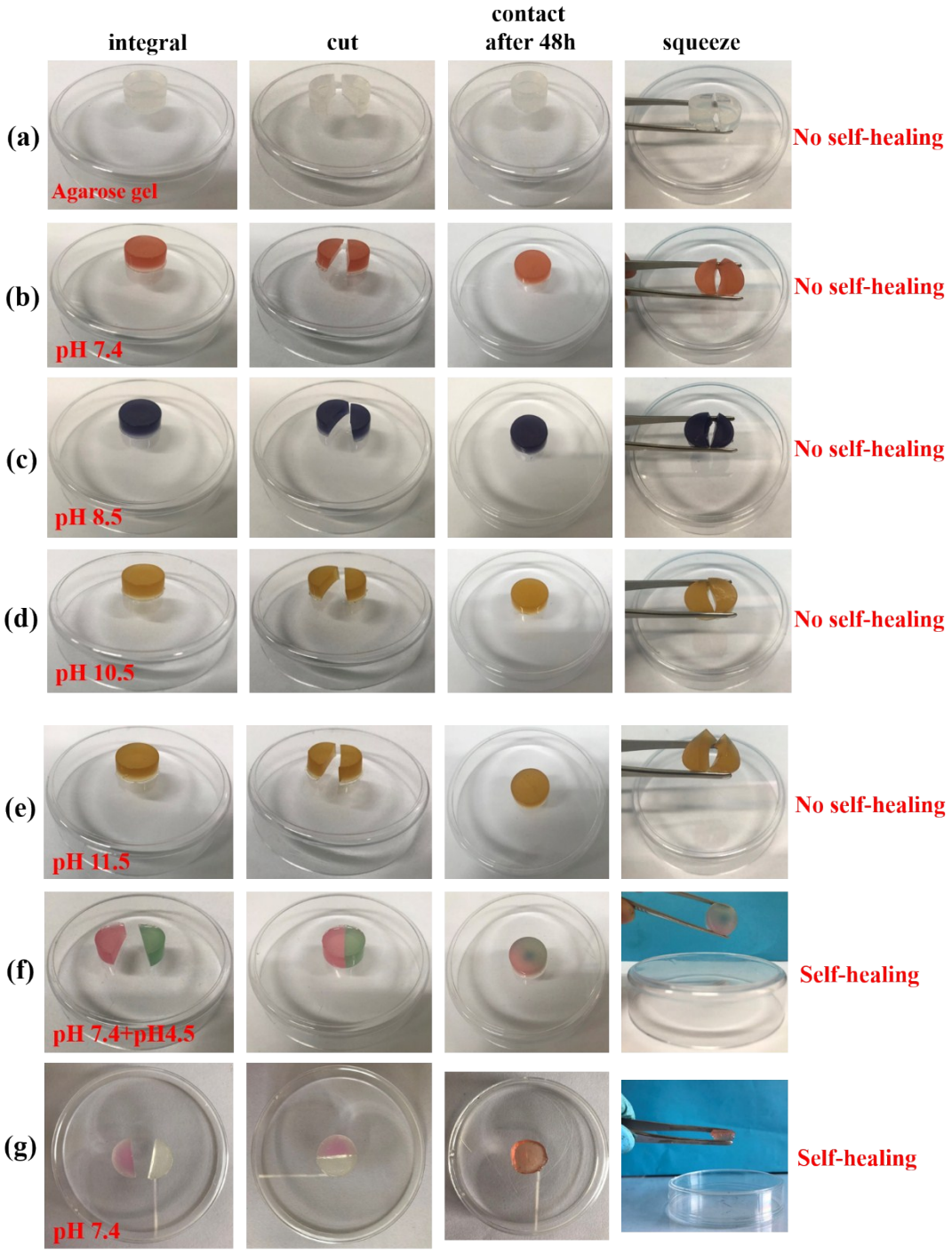

Figure S12**.** Self-healing tests of the Aga or DN gels formed in aqueous buffers of pH (a) Aga gel, (b) 7.4, (c) 8.5, (d) 10.5, (e) 11.5, (f) 7.4+4.5, and (g) DN gel formed in an aqueous buffer solution of pH 7.4 after the addition of a small volume of an aqueous buffer solution of pH 4.5 (The concentration of SA-CHO is 8 w/v%).

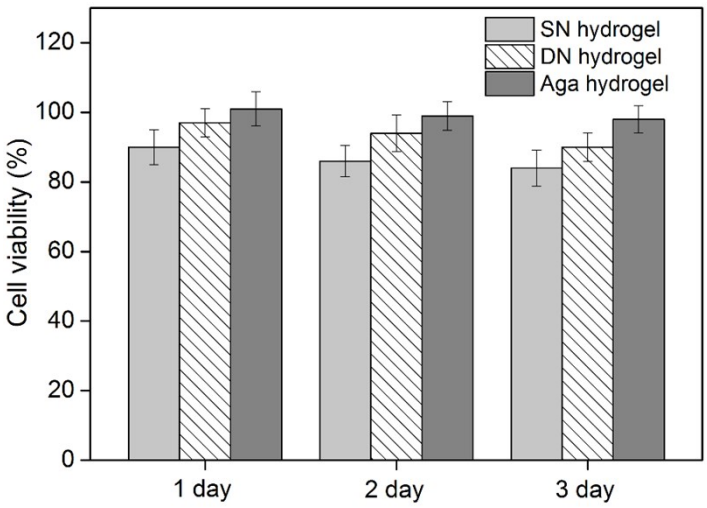

Figure S13**.** Cytotoxicity test of SA-CHO SN, DN, and Aga gels leachable solutions with L929 fibroblast cells. (Values were presented as mean ± standard deviation, n = 3).

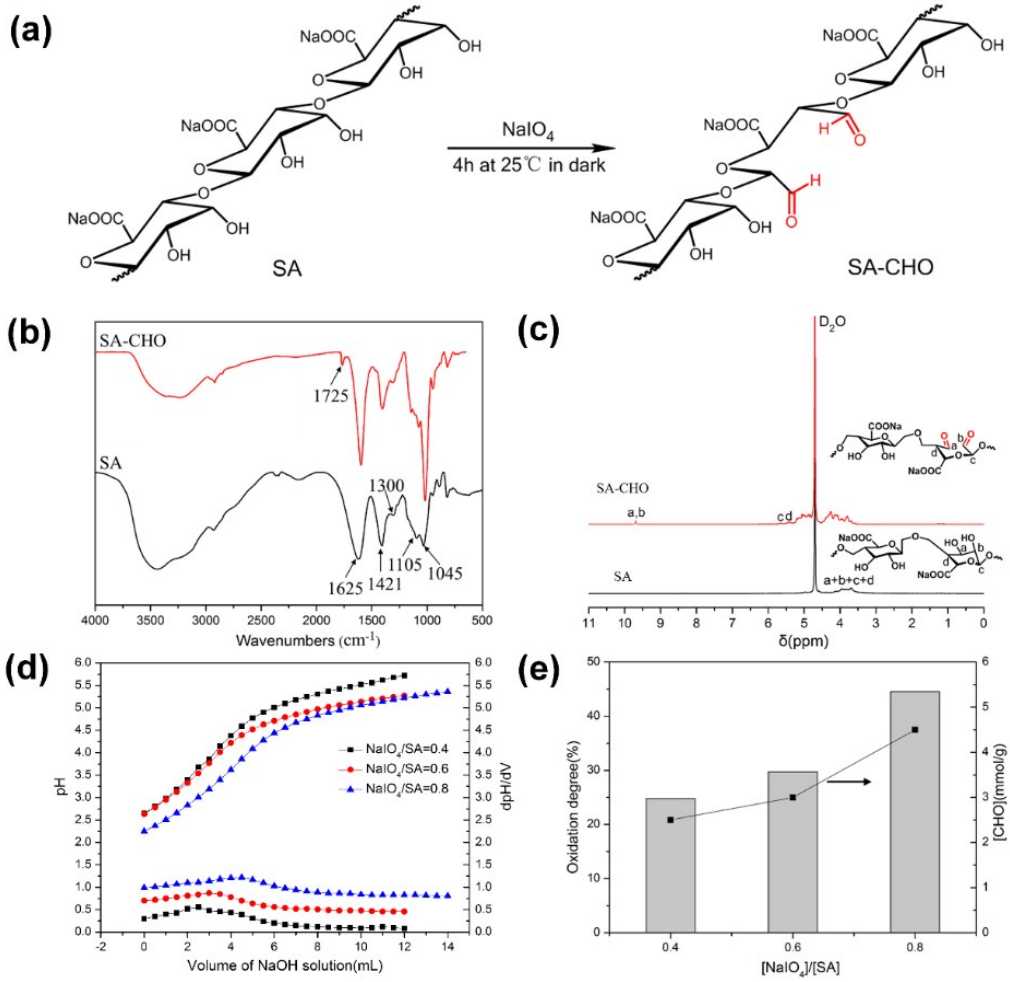

Figure S14. Synthesis and characterization of SA-CHO. (a) Schematic and structure of SA-CHO; (b) FTIR spectra of SA, and SA-CHO; (c) ^{1}HNMR spectra of SA, and SA-CHO; (d) Hydroxylamine hydrochloride potentiometric titration of various SA-CHO samples; (e) Oxidation degree (mol%)

and aldehyde group content of SA-CHO at different ratio of [$NaIO_4$]/[SA].

Note: [$NaIO_4$], and [SA] refer to the molar amount of $NaIO_4$, and saccharide repeating units of SA, respectively.

SA-CHO was obtained through the oxidation of SA by using NaIO4 (Figure S14a) and Synthesis of SA-CHO was verified by FTIR, and ^{1}HNMR, as shown in Figure S14b, c. As can be seen from Figure S14b, for the raw material SA, the typical absorption peaks of polysaccharide structure were about 1300 (O-C-H and C-C-H stretching vibration), 1105 (C-O stretching vibration), and 1045 cm^{-1} (C-C and C-O stretching vibration of pyranose rings). The peaks appearing at 1421 and 1625 cm^{-1} were attributed to the symmetric and asymmetric stretching vibration of carboxylate, respectively. In contrast to the absorption curve of SA, a new peak at 1725 cm^{-1} could be observed in the spectrum of SA-CHO, being ascribed to the CHO stretching vibration, which revealed effective fabrication of SA-CHO. The oxidation of SA was also certified by ^{1}HNMR in Figure S14c. Compared with the 1HNMR spectrum of SA, new peak at δ 9.75 (peak a, b), was clearly explored confirming the successful preparation of the SA-CHO. The oxidation degree of SA-CHO was determined by Hydroxylamine hydrochloride potentiometric titration. The titration curve was displayed in Figure S14d. At titration endpoint, the volume of NaOH solution could be acquired by peaks of the first differential peak of the titration curve. As concluded in Figure S14e, OD went up from 24.8 to 44.6% with the [NaIO4]/[SA] molar ratio increasing from 0.4 to 0.8. The [CHO] was 2.5, 3.0, and 4.5 mmol/g, corresponding to the [NaIO4]/[SA] molar ratio 0.4, 0.6, and 0.8. In this work, the SA-CHO with 44.6% of OD value was used to fabricate hydrogels.

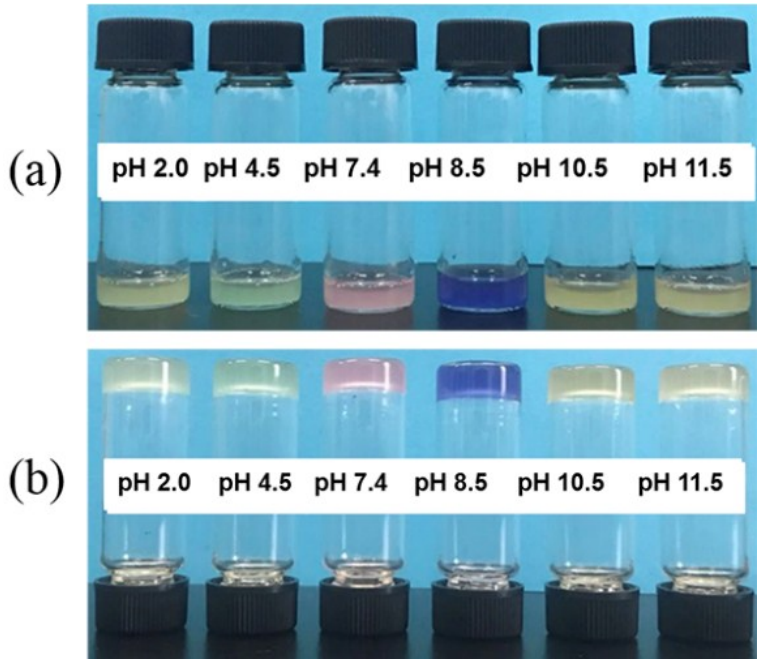

Figure S15**.** Tube inversion tests demonstrating the fabrication of SA-CHO/Aga DN gels (10% DN gel) within the pH range 2.0-11.5. (a) Before the gelation. (b) After the gelation. Different coloration is attributed to the existence of some traces of dye.

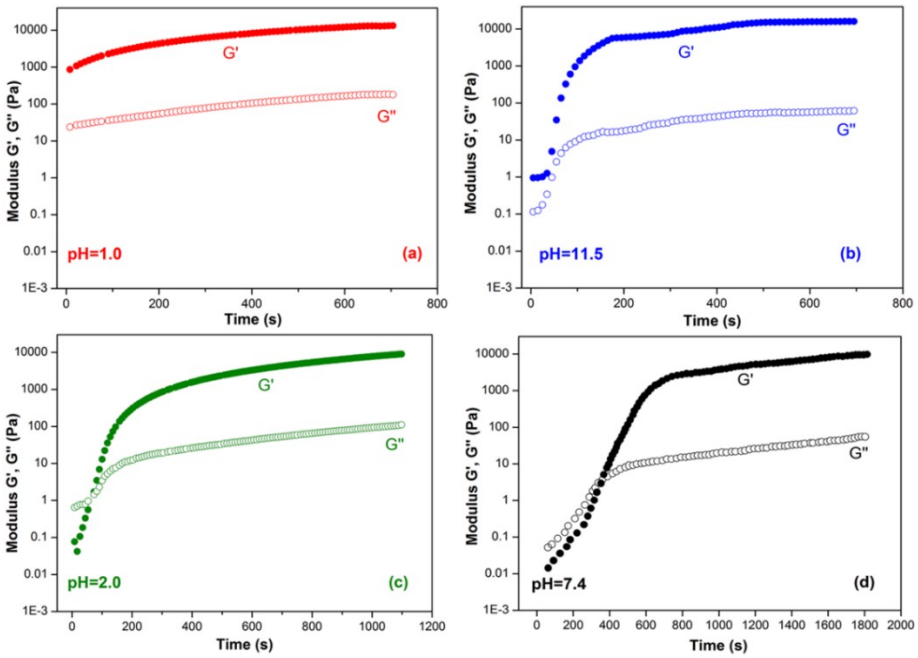

Figure S16**.** Temporal changes of the G' and G'' during the formation of SA-CHO/Aga DN gels (10% DN gels) at 50 ℃ in PBS solution with various pH values (a) 1.0, (b) 11.5, (c) 2.0, and (d) 7.4.

In aqueous solution, the formation of the Schiff's base was greatly affected by pH. Here, the pH-controlled formation of the DN hydrogels was researched via tube inversion

(Figure S15) and rheology experiments (Figure S16) with the pH range from 2.0 to 11.5, using various PBS. In order to eliminate the effect of the temperature-controlled formation of the Aga network on the formation of Schiff's base linkages, the above experiments were carried out at 50 ^{0}C preventing the forming of Aga hydrogel before forming SA-CHO hydrogel network. The appearance of the hydrogel samples after the gelation at all six values of pH is shown in Figure S15; trace of dye was added to each pair of SA-CHO/Aga solution before mixing, so that every hydrogel sample at different pH is recognized according to its color. Besides, the temporary changes of the elastic modulus G' and viscous modulus G'' during the gelation were characterized by rheology at four different values of pH as displayed in Figure S16. At extreme pH values 1.0, and 11.5, gels were rapidly formed within 1 min with G' being bigger than G'' at the beginning. At pH value 2.0, and 7.4, G'' was bigger than G', indicating a sol state of the system at the beginning. As the acylhydrazone bonds formed, the G' exceeded the G'', corresponding to the formation of a gel. In Figure S16c, d, the intersection point of the curves of G' and G'' was defined as the gelation point, which was considered the transformation time from sol to gel.

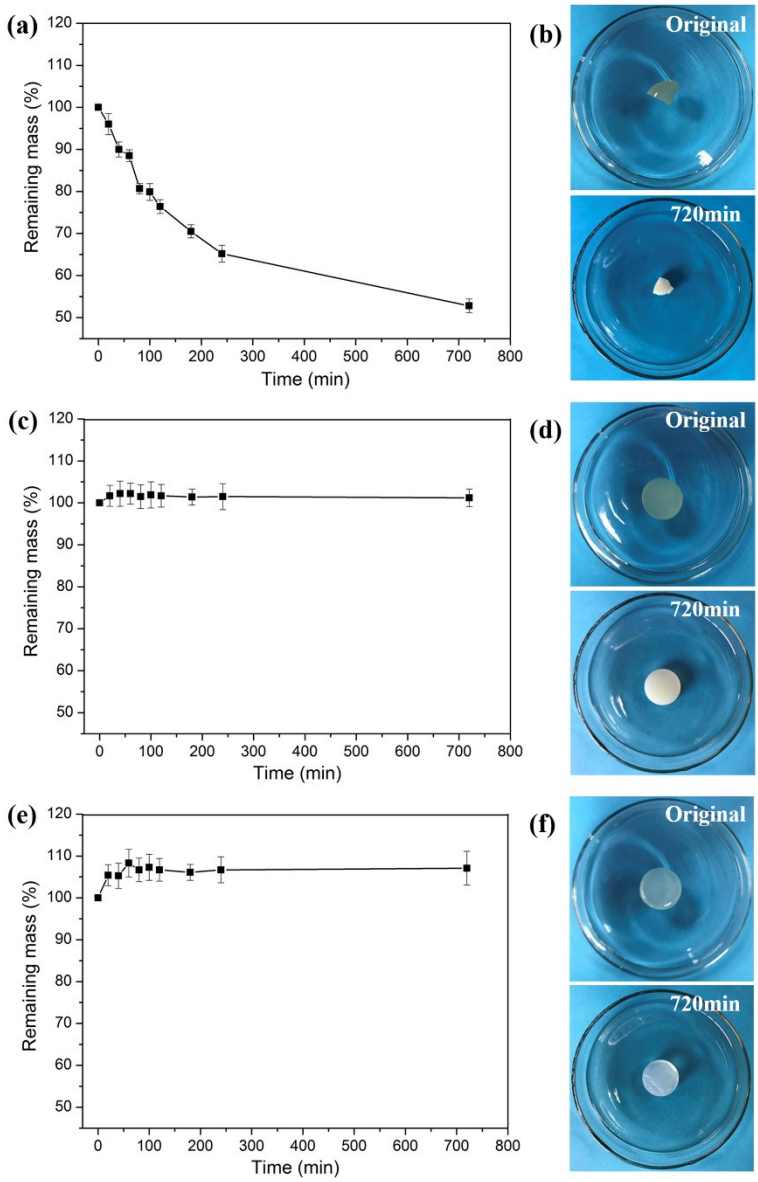

Figure S17. Swelling and stability properties of the gels in acidic condition (pH=1). (a) The swelling behavior of the SA-CHO gel. (b) Pictures of the SA-CHO gel's form change. (c) The swelling behavior of the DN gel. (d) Pictures of the DN gel's form change. (e) The swelling behavior of the Aga gel. (f) Pictures of the Aga gel's form change. (Values were presented as mean ± standard deviation, n = 4).

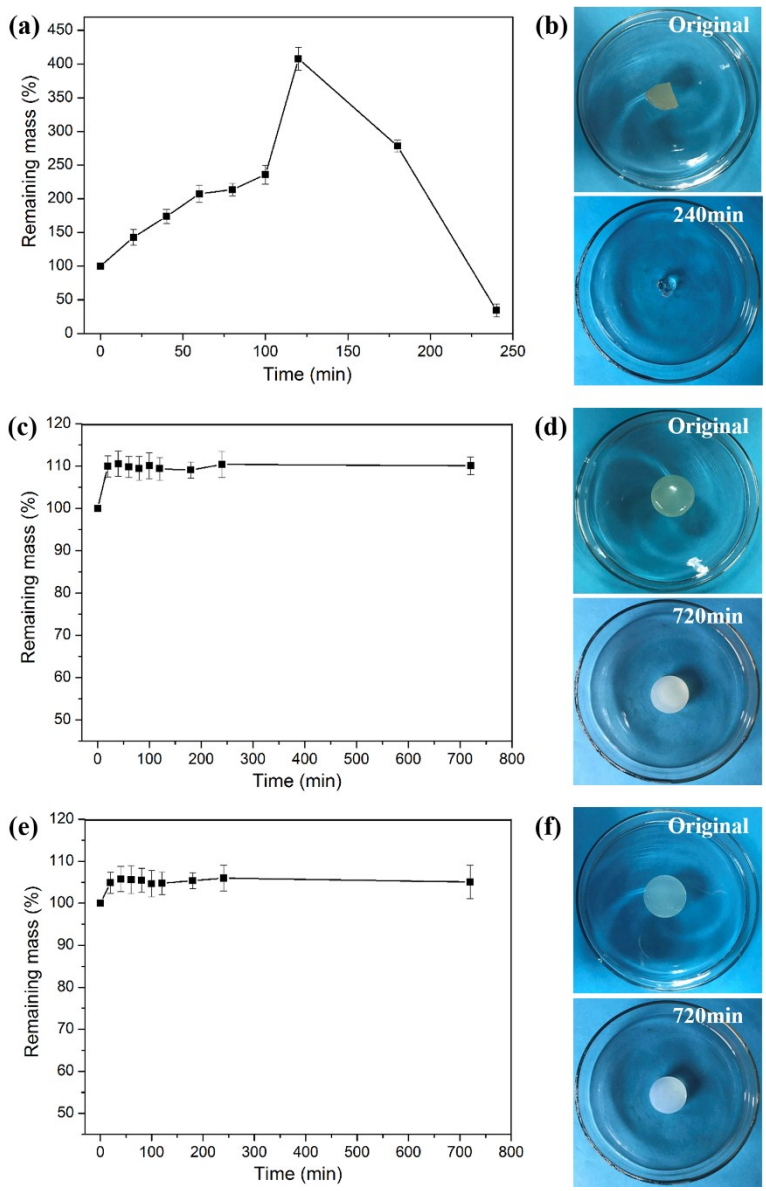

Figure S18. Swelling and stability properties of the gels in DI water. (a) The swelling behavior of the SA-CHO gel. (b) Pictures of the SA-CHO gel's form change. (c) The swelling behavior of the DN gel. (d) Pictures of the DN gel's form change. (e) The swelling behavior of the Aga gel. (f) Pictures of the Aga gel's form change. (Values were presented as mean ± standard deviation, n = 4).

As biomedical materials, it is very important to adapt to a complicated surroundings in vivo and remain a steady state in acid-base conditions generated by microbe. Hence, the swelling characteristics of SA-CHO, DN, and agarose hydrogels in acidic condition were examined (Figure S17). As can be seen from Figures S17a, due to the dynamic reaction of acylhydrazone bond, SA-CHO SN hydrogel in acidic solution presented a fast disintegration with approximately 50% of mass loss in 720 min. Meanwhile, with

the fast degradation of the SA-CHO hydrogel, the crack appeared in the gel, accompanied by shrunken and whiten gel appearance, and this was attributed to the dehydration of SA molecular chains in acidic condition (Figure S17b). Oppositely, the SA-CHO/Aga DN, and agarose hydrogels could remain their initial state and intact gel structures, followed by a slight swelling until the equilibrium was achieved with the 102%, 108% of remaining mass for SA-CHO/Aga DN, agarose hydrogels, respectively (Figures S17c-f). Similarly, the swelling behaviours of SA-CHO, DN, and agarose hydrogels in DI water were also researched. Figure S18a shows the swelling properties of the SA-CHO hydrogel in DI water, and in the initial 120 min, an increase of remaining mass was observed with the 400% of remaining mass and this was ascribed to the initial swelling of the hydrogels. Then, a sharp decrease of gel mass can be seen, attributed to the rapid disintegration of reversible acylhydrazone bond in the gel. It is noteworthy that compared with the appearance of SA-CHO hydrogel in acidic solution after the swelling, the SA-CHO hydrogel in DI water presents a transparent and swollen form rather than a shrunken and whiten form, and this is due to the excellent water absorption of SA in DI condition (Figure S18b). Oppositely, the SA-CHO/Aga DN, and agarose hydrogels could keep their primary forms and intact gel structures in DI water, accompanied by a slight swelling until the equilibrium was attained with the 110%, 106% of remaining mass for SA-CHO/Aga DN, agarose hydrogels, respectively (Figures S18c-f). Also due to the excellent water absorption of SA in DI condition, the SA-CHO/Aga DN hydrogel has the higher remaining mass compared with the DN hydrogel in acidic solution.

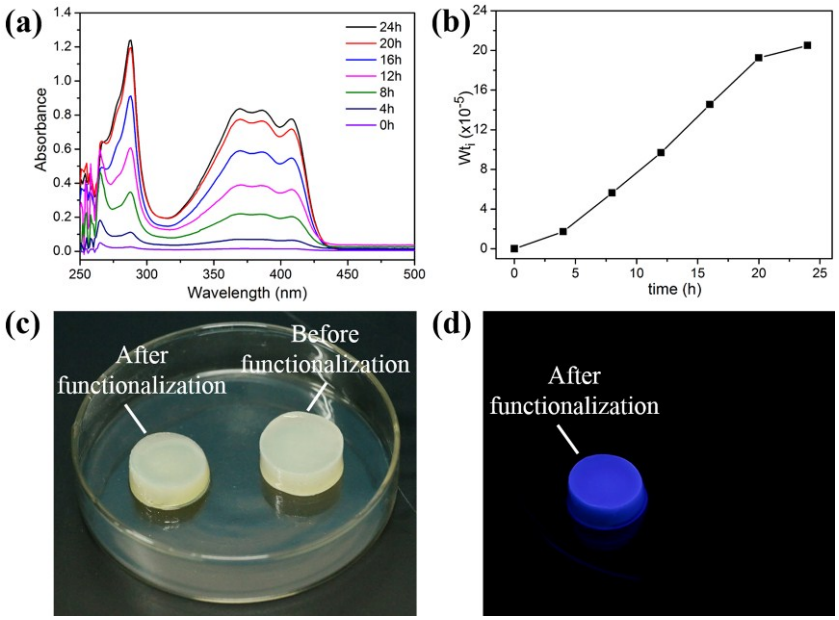

Figure S19**.** (a) UV-visible spectra of the gel after functionalization for different time, (b) Fluorescence yield (W_{ti}) of aminopyrene in DN gel functionalized for different time. Pictures of DN gels under visible light (c), and UV-visible light (d).

It was mentioned that aldehyde group with higher activity can be readily functionalized for various bio-applications including cell diagnosis, drug delivery, and fluorescence probing. Hence, unreacted aldehyde groups in the DN hydrogels can be utilized for further functionalization of the SA-CHO/Aga DN hydrogels. In order to distinctly demonstrate this, fluorescent aminopyrene-NH_2 was grafted onto the hydrogel via CHO-NH_2 Schiff base in DMF. After that, the DN hydrogel was examined by laser confocal microscopy (Figure S19). The distinct blue color of the aminopyrene observed along the hydrogels confirmed the perfect functionalization. Besides, the UV-visible spectra of the DN hydrogel after functionalization for different time were displayed in Figure S19a. The intensity of the absorption peaks of aminopyrene at 287 nm gradually increased with the time lengthening, and after functionalization for 20 h, the intensity maintained nearly unaltered, manifesting the complete reaction of CHO-NH_2 Schiff base. The corresponding fluorescence yields (Wt_i) of aminopyrene in SA-CHO/Aga DN hydrogels functionalized for different time were summarized in Figure S19b. After the complete functionalization of DN hydrogel for 20 h, the fluorescence yield was approximately 19.25×10^{-5}. Pictures of the hydrogels before and after functionalization were showed in Figure S19c, d. Compared with the original SA-CHO/Aga DN hydrogel, the functionalized DN hydrogel exhibits strong blue fluorescent under the ultraviolet light, as shown in Figure S19d. The aldehyde can also interact with

numerous other active groups, like amino group, hydroxyl group, and so on. Based on these reactions, the SA-CHO/Aga DN hydrogels could be conveniently functionalized with bioactive drugs or proteins.

References:

1 B. Balakrishnan and A. Jayakrishnan, *Biomaterials*, 2005, **26**, 3941-3951.

2 Z. Wei, J. H. Yang, Z. Q. Liu, F. Xu, J. X. Zhou, M. Zrinyi, Y. Osada and Y. M. Chen, *Adv. Funct. Mater.*, 2015, **25**, 1352-1359.

3 Q. X. Hou, W. Liu, Z. H. Liu, B. Duan and L. L. Bai, *Carbohydr. Polym.*, 2008, **74**, 235-240.

4 C. J. Fan, C. Zhang, L. Q. Liao, S. Li, W. P. Gan, J. P. Zhou, D. A. Wang and L. J. Liu, *J. Mater. Chem. B*., 2015, **3**, 6618-6625.